THE IIOAB JOURNAL

VOLUME 6 : NO 3 : OCTOBER 2015 : ISSN 0976-3104

Institute of Integrative Omics and Applied Biotechnology Journal

Dear Esteemed Readers, Authors, and Colleagues,

I hope this letter finds you in good health and high spirits. It is my distinct pleasure to address you as the Editor-in-Chief of Integrative Omics and Applied Biotechnology (IIOAB) Journal, a multidisciplinary scientific journal that has always placed a profound emphasis on nurturing the involvement of young scientists and championing the significance of an interdisciplinary approach.

At Integrative Omics and Applied Biotechnology (IIOAB) Journal, we firmly believe in the transformative power of science and innovation, and we recognize that it is the vigor and enthusiasm of young minds that often drive the most groundbreaking discoveries. We actively encourage students, early-career researchers, and scientists to submit their work and engage in meaningful discourse within the pages of our journal. We take pride in providing a platform for these emerging researchers to share their novel ideas and findings with the broader scientific community.

In today's rapidly evolving scientific landscape, it is increasingly evident that the challenges we face require a collaborative and interdisciplinary approach. The most complex problems demand a diverse set of perspectives and expertise. Integrative Omics and Applied Biotechnology (IIOAB) Journal has consistently promoted and celebrated this multidisciplinary ethos. We believe that by crossing traditional disciplinary boundaries, we can unlock new avenues for discovery, innovation, and progress. This philosophy has been at the heart of our journal's mission, and we remain dedicated to publishing research that exemplifies the power of interdisciplinary collaboration.

Our journal continues to serve as a hub for knowledge exchange, providing a platform for researchers from various fields to come together and share their insights, experiences, and research outcomes. The collaborative spirit within our community is truly inspiring, and I am immensely proud of the role that IIOAB journal plays in fostering such partnerships.

As we move forward, I encourage each and every one of you to continue supporting our mission. Whether you are a seasoned researcher, a young scientist embarking on your career, or a reader with a thirst for knowledge, your involvement in our journal is invaluable. By working together and embracing interdisciplinary perspectives, we can address the most pressing challenges facing humanity, from climate change and public health to technological advancements and social issues.

I would like to extend my gratitude to our authors, reviewers, editorial board members, and readers for their unwavering support. Your dedication is what makes IIOAB Journal the thriving scientific community it is today. Together, we will continue to explore the frontiers of knowledge and pioneer new approaches to solving the world's most complex problems.

Thank you for being a part of our journey, and for your commitment to advancing science through the pages of IIOAB Journal.

Yours sincerely,

Vasco Azevedo

Vasco Azevedo, Editor-in-Chief
Integrative Omics and Applied Biotechnology
(IIOAB) Journal

Prof. Vasco Azevedo
Federal University of Minas Gerais
Brazil

Editor-in-Chief

Integrative Omics and Applied Biotechnology (IIOAB) Journal Editorial Board:

ISSN: 0976-3104
REGULAR ISSUE
Shaik and Masilamani

THE IIOAB JOURNAL

RESEARCH ARTICLE OPEN ACCESS

A ROBUST DIGITAL IMAGE WATERMARKING BASED ON SINGULAR VALUE DECOMPOSITION AND TABU-SEARCH

Ayesha Shaik* **and Vedhanayagam Masilamani**

Department of Computer Engineering, IIITD & M Kancheepuram, Chennai, INDIA

ABSTRACT

Digital Watermarking has become an essential tool for protecting copyrights of digital data. A singular value decomposition (SVD) and Tabu Search based digital image watermarking method has been proposed. In this approach, the singular value of the original data has been modified using multiple scaling factors for embedding the watermark image. These multiple scaling factors are generated using a meta-heuristic approach known as Tabu search. The Watermarked image obtained by the proposed approach is robust under various attacks such as rotation, cropping, JPEG compression, Histogram equalization, Average filtering and Gaussian noise.The experiment done on the standard benchmark data set shows the proposed algorithm which uses Tabu Search is more robust than the best known algorithm which uses Genetic Algorithms (GA).

Received on: 7th-April-2015
Revised on: 8th-May-2015
Accepted on: 4th-June-2015
Published on: 1st-July-2015

KEY WORDS

Watermarking; Singular Value Decomposition; Tabu Search; Meta-Heuristic; Multiple Scale factors; Robust;

***Corresponding author:** Email: ayeshanoormd@gmail.com; masila@iiitdm.ac.in **Tel:** +91-44-27476391/ 6346

INTRODUCTION

The rapid development of the Internet and availability of networked computers has made the distribution of multimedia data very fast and convenient without losing information. The consequences of such applications lead to modification and distribution of illegal data easier for the unauthorized parties. To overcome these problems, digital watermarking technique came into existence. Digital watermarking is a technique of inserting copyright (watermark) into the digital data, such as text, audio, image and video, etc. The applications of digital image watermarking are: copyright authentication, data authentication, user identification, copy protection and automated monitoring [1, 35]. The watermarking techniques can be classified based on the domain (as Spatial domain and Transform domain), the strength of the watermark (as fragile, semi-fragile and robust), visibility of the watermark (as visible and invisible) and the requirement of the original image while extracting the watermark (as Non-Blind and Blind) [2]. Also the requirements of digital watermarking such as transparency, fidelity, robustness and capacity or data payload of the watermark have been discussed.

Secure Spread spectrum watermarking has been presented in [3] and the methodology can be generalized to audio, video and multimedia data, where the watermark is independent and identically distributed Gaussian random vector and embedded imperceptibly into most significant spectral components of the original image. This method is robust to signal processing operations and common geometric distortions provided that the original image is available, i.e. the method discussed is Non-Blind watermarking. The watermarking scheme need to be adaptive in order to be robust as discussed in [4], and it should identify and embed the watermark in most significant features of the original image.

In visible watermarking, watermark is visible, because the watermark is overlaid on the original image. The watermark needs to be overlaid in a way that it has to be difficult to remove the watermark which can be a text or logo. In invisible watermarking the watermark is embedded imperceptibly into the original image. One of the simple invisible watermarking schemes is modifying the LSB plane of the original image with the message bits that need to be embedded [5].

THE IIOAB JOURNAL
ISSN: 0976-3104

Spatial domain watermarking is simple and has advantages of easy implementation, low complexity. Generally the spatial domain techniques are not robust, they are fragile. Different variations and improvements of this method are also available. In spatial domain watermarking, the embedded watermark can't resist image processing operations or attacks. The Frequency domain watermarking is performed by inserting the watermark into the magnitude of the coefficients in the frequency domain. Existing transform domain watermarking techniques include: FFT (Fast Fourier Transform), DCT (Discrete Cosine Transform), DWT (Discrete Wavelet Transform), SVD (Singular Value Decomposition) and hybrid (Combination of the above transforms).

In Transform domain watermarking techniques, DWT [6, 12-19, 21-23] and SVD [7, 20] watermarking techniques have been proposed. Another watermarking technique using principal component analysis (PCA) has been discussed in [8], where the watermark is embedded in the highest energy coefficients (most significant features). DCT domain watermarking is classified into global and block-based DCT watermarking. In the global DCT scheme, a watermark is embedded in perceptually significant portion of the original image [9] and the watermarking schemes based on DCT and its variations has been discussed in [24-28]. A hybrid watermarking technique using a combination of both DWT and SVD transforms for user authentication in biometrics is proposed in [10]. DWT and the SVD watermarking scheme is proposed in [29]. An image adaptive watermarking scheme that uses wavelet for watermarking, where the watermark is embedded in the portion of the image that exhibits high tolerance towards the modification is discussed in [11]. The rotation, scale and translation invariant watermarking of a digital image with log polar mapping and phase correlation is proposed in [30]. Another reversible transform used for watermarking is Walsh-Hadamard Transform (WHT) and this technique has been presented in [31, 32].

Several digital image watermarking methods have been proposed previously. In [25], DCT watermarking method for sub bands of a digital image has been proposed. In the DWT watermarking scheme, the watermarking method is same as in DCT, the difference is in the process of transforming the original image in its frequency domain [36]. Different DWT watermarking schemes have been proposed. One of those is [13], at multiple resolutions the watermark is embedded in all high pass bands in a nested manner. In order to consider HVS factor, [14, 15] improved this technique by adding HVS factor. A dual domain watermarking technique for image authentication and compression is presented in [37], where the watermark is generated using DCT domain, and DWT domain is used to insert the watermark.

If the watermark is embedded in low frequency components of the image, then it is robust to low pass filtering, lossy compression and geometric distortions and if the watermark is embedded in the high frequency components of the image then it is robust to contrast and brightness adjustments, gamma correction, histogram equalization and cropping. In order to achieve the overall robustness of the watermarked image, multiple watermarks are embedded in low and high frequency components of the DWT transform [18]. Optimal wavelet based watermarking scheme is presented in [38], where a binary logo is used as watermark and it is inserted in all four sub bands of DWT transform with variable scaling factors in different sub bands i.e., high scaling factor for an LL sub band and low scaling factor for other three sub-bands. In [39], an improved watermarking scheme is proposed where the watermark is embedded in the SVD domain of four sub bands (LL, LH, HL, HH) of DWT transformed image.

The DFT domain watermarking technique utilizes a circular symmetric watermark to embed in the 2-D DFT domain of the original image [41]. As the watermark is circular in shape, it is robust to geometric rotation attack. Here it discusses that the scaling in spatial domain leads to inverse scaling in the frequency domain and rotation in spatial domain leads to the same rotation in the frequency domain. DFT is resistant to translation and cropping [40], Circular shifts in spatial domain do not have an effect on the magnitude of the Fourier spectrum. In above both papers, watermarking the low frequency components have some visible effect in spatial domain, and high frequency components will be removed during JPEG compression. So, embedding the watermark in mid frequencies will be better. In DFT watermarking, the watermark can be embedded either in magnitude or phase information. A DFT watermarking technique which uses phase information for embedding the watermark presented in [43], is robust to image contrast operation. Another DFT watermarking in which multiple watermarks have been embedded in low and high frequency bands are discussed in [42]. A RST resilient watermarking is presented in [44], in which watermark is embedded in the magnitude information of the re-sampled Fourier spectrum by log-polar mapping. This is not robust to cropping and weak robust to JPEG compression. Hadamard Transform based watermarking that modifies the high frequency Hadamard coefficients for embedding the watermark is proposed in [45]. A watermarking technique that uses a multi-resolution transform and Complex-Hadamard transform is presented in [46]. The multi resolution Hadamard transform is applied first, then Complex Hadamard transform is applied and the watermark is embedded in the phase component as it is more robust to

THE IIOAB JOURNAL
ISSN: 0976-3104

noise compared to amplitude modulation. An improved watermarking technique for JPEG images has been presented in [47].

In case of image watermarking, illegal tampering of the watermark should not destroy or transfer the watermark to another valid signature and it should maintain the quality of the image as well. So, in [48] two perceptual based watermarking techniques are proposed: Block-based DCT and Multi resolution wavelet framework and it provides good results for image transparency and robustness, which are the basic requirements of an effective watermarking scheme. Multi Resolution WHT (MR-WHT) and SVD based robust watermarking scheme for copyright protection is presented in [49], the image is first decomposed into sub-bands using MR-WHT and the middle singular values of the high frequency band at the coarsest and finest level are modified by the singular values of the watermark.

A new watermarking scheme with the combination of Fast WHT (FWHT) and DCT has been proposed in [50]. An adaptive image watermarking technique based on just-noticeable difference (JND) and Fuzzy Interference System (FIS) optimized with Genetic Algorithm (GA) is presented in [51]. To embed the watermark it utilizes the JND profile of the image and to improve watermark extraction performance FIS with optimized GA is used. It is robust to image manipulation attacks. In the image watermarking one of the key problems is how to hide the robust gray scale or color watermarks which is discussed in [52]. A block based watermarking scheme using SVD, where the watermark is inserted in right singular values of each block of the original image is proposed in [53].

In SVD watermarking technique the scaling factor of the watermark is maintained constant [33]. In [34], it is suggested that multiple scale factors can be considered because using constant scale factor may not be efficient in some cases. In [20], a digital watermarking scheme based on singular value decomposition and a Tiny genetic algorithm (for finding optimum scale factors) is proposed. In this paper, an SVD watermarking scheme that uses Tabu search, which is a meta-heuristic approach to find optimal scale factors to watermark the singular values of the original image is proposed.

MATERIALS AND METHODS

In this section, basic SVD based watermarking is explained in detail. Then the concept of Tabu search is discussed and how it is used to determine proper multiple scale factors for the singular values of the original image is described.

SVD based watermarking

In most of the image processing applications, image can be perceived as a matrix with non-negative scalar values. The SVD of an image F of size M x M is calculated as, $F = U\ S\ V^T$, where U and V are orthogonal matrices of size M x M and M x M respectively, and S is a diagonal matrix of size M x M i.e., S = diag (ei) where ei 's are the singular values arranged in decreasing order with i = 1, 2, 3, ..., M. Singular values of an image will have most of the energy concentrated in the beginning of the diagonal matrix as they are arranged in decreasing order. It contains the luminance values of the image and the slight modification done to the singular values will not affect the original image visual quality. So, for SVD watermarking the singular values are used for embedding the watermark. SVD of image F can be written as:

$$F = \sum_{i=1}^{r} u_i\ s_i\ v_i^T$$

Here r specifies the rank of the matrix F, ui and vi are left and right singular vectors respectively. From [7], The SVD watermarking is as follows: First, the SVD operation is performed on the original image, F resulting in three matrices U, S and V. Then, a watermark is embedded in diagonal matrix, S as S' = S + α W, where α is used to scale the watermark strength and SVD operation is employed on S' obtain three matrices U_W, S_W and V_W. The watermarked image, F_W is obtained by multiplying three matrices U, S_W and V^T.

$F = U\ S\ V^T$;
S' = S + α.W, where α.W is point wise multiplication, i.e., $\alpha\ W = (\alpha_1 W_1, \alpha_2 W_2, .. \alpha_n W_n)^T$;
$S' = U_W\ S_W\ V_W^T$;
$F_W = U\ S_W\ V^T$;

By performing the inverse operation of the watermarking, watermark extraction can be done. F_W^* is possibly modified watermarked image.

$F_W^* = U^*\ S_W^*\ V_T^*$;
$D^* = U_W\ S_W^*\ V_W^T$;

THE IIOAB JOURNAL
ISSN: 0976-3104

W* = (1/ α) (D* - S);
The verification of the watermark can be done by correlating with the inserted watermark.

The scaling vector α plays an important role in obtaining robustness. Choosing the optimal vector α using Brute-Force technique requires an exponential amount of time. Hence, it is better to use soft computing technique to find optimal or close to optimal in polynomial time. [20] uses Genetic Algorithms (GA) to find optimal vector α to get best robustness. In this paper, we use Tabu Search to find optimal vector α and the experiment done on the standard data set shows that Tabu Search gives more robustness than the GA in watermarking.

Tabu-search

Tabu Search was created by Fred W. Glover in 1986. It is a meta heuristic algorithm used for solving combinatorial optimization problems. In this paper, Tabu Search is used for optimizing the scaling factors. In [20], the authors have used Tiny GA (Genetic algorithm) for optimizing the scaling factors with small population size (ten chromosomes), little number of generations and simple fitness.

When Tabu Search is used to solve the problem, the following need to be considered: 1) Representation of solution for the problem, 2) Initial Solution, 3) Generating Candidate solutions, 4) Fitness evaluation function, 5) Tabu List to store the solutions for reducing cycles and 6) Termination criteria. Tabu Search usage can reduce the effort of computation required to generate the optimized scaling factors for watermark embedding.

Representation of the Solution: The solution, which is a vector of scaling factors to embed the watermark in the diagonal matrix can be represented as vector a = (a_1, a_2, a_3. . . a_n), where $a_i \in [0, 1]$, $1 \le i \le n$ and n x n is the dimension of diagonal matrix.

Initial Solution: Randomly generated vector of scaling factors is given as initial solution. It is assumed as the best solution (S_{best}) available till better solution is obtained.

Candidate Solutions generation: Given initial random solution, a = (a_i), where $a_i \in [0, 1]$, $1 \le i \le n$ and n x n is the dimension of diagonal matrix. Candidate solutions (CS_i) are generated as follows:

CS_i = (a_1, a_2, . . ., max (a_i, a_{i+1}), k_i , a_{i+2}, ... , a_{n-1}) ; where $a_i \in [0, 1]$; $1 \le i \le n-1$. The value of k_i is determined by the following Algorithm1, Scale (a_i, a_{i+1}) i.e., k_i = Scale (a_i, a_{i+1}) as follows:

Algorithm 1 Scale(a_i, a_{i+1})

```
initialize w=0.2
if a_i < a_{i+1} then
  lc = w.a_i + (1-w). a_{i+1}
else
  lc = w.a_{i+1} + (1-w). a_i
end if
if lc ≤ 0.2 then
  k_i=1-lc
else
  if lc ≥ 0.8 then
    k_i= lc
  else
    if 0.2 < lc ≤ 0.4 then
      lc = lc-0.2
      k_i= 1-lc
    else
      if 0.6≤ lc ≤ 0.8 then
        lc = lc + 0.2
        k_i = lc
      else
        lc = lc - 0.4
        k_i = 1- lc
      end if
    end if
  end if
end if
```

The candidate solution CS_i generated in the i^{th} iteration from the candidate solution in the previous iteration by changing i^{th} element a_i with the maximum of a_i and a_{i+1} i.e. max(a_i,a_{i+1}) and $(i+1)^{th}$ element by k_i = Scale(a_i, a_{i+1}). The algorithm that computes Scale(a_i,a_{i+1})

THE IIOAB JOURNAL
ISSN: 0976-3104

uses a parameter w, and w is initialized 0.2. The objective of Scale() function is to find the convex linear combination of a_i and a_{i+1} and the resultant value k is to be a high value in the range [0, 1]. The k found by the algorithm is more than 0.8 and less than 1.If different w is chosen, then steps in the algorithm needs to be modified so that $0.8 \leq k \leq 1$. The reason why we need to keep k in the range [0.8, 1] is that high value of k gives more robustness.

Fitness Evaluation: Fitness function is defined as a function of imperceptibility and robustness. It is used to balance the main requirements of watermarking i.e., imperceptibility and robustness.

$$Fitness = f(Imperceptibility, Robustness)$$

Fitness is measured for all the candidate solutions generated, F = (f_1, f_2, f_3, ..., f_{n-1}) and fitness for the initial solution is also measured, F_{best}. Candidate solution with minimum fitness (F_{min}) is selected as solution for the next iteration. If the fitness F_{min} is less than the best fitness, F_{best} then the candidate solution with F_{min} is selected as the best solution.The imperceptibility is measured as a normalized correlation between the original image and the watermarked image to determine the visual quality of the watermarked image. Robustness means that when the watermarked image is attacked, the inserted watermark has to be extracted with some distortion. Imperceptibility and robustness are defined by formulas as follows [20]:

$$Imperceptibility = NC(F, F_w)$$

$$Robustness = \frac{N}{\sum_{i=1}^{N} NC(W,W_i^*)}$$

$$NC(X, X^*) = \frac{\sum_i \sum_j X(i,j)X^*(i,j)}{\sqrt{\sum_i \sum_j X(i,j)^2}\sqrt{\sum_i \sum_j X^*(i,j)^2}}$$

where X and X* are the original and processed watermarked image respectively;
W, W_i* are the inserted and the extracted watermarks; N is the number of attacks considered;
F and F_W are the original and watermarked image.

Tabu list: Tabu list is used to store the candidate solutions that are best and used as the solution for the next iteration. If the candidate solution to be updated for the next iteration is already present in tabu list, then the next candidate solution with minimum fitness is selected for the next iteration. Tabu list is used to for removing cycles in the solutions, by neglecting the updated solutions in Tabu List. The solutions in the Tabu List are updated in a FIFO manner.

Termination criteria: If the number of iterations is met or if the same fitness value is being repeated for some number of iterations, then the algorithm is terminated.

Proposed work

The proposed watermarking algorithm is as shown in **Figure-1**. SVD transform is applied to the original image F i.e. $F = U S V^T$, where U and V are orthogonal matrices and S is a diagonal matrix. The diagonal matrix, S is modified by the watermark image with the initial scaling factor, α = (α_1, α_2, ..., α_N), where N x N is the size of the diagonal matrix as follows:

$S' = S + \alpha.W$, where α.W is point wise multiplication, i.e., $\alpha W = (\alpha_1 W_1, \alpha_2 W_2, .. \alpha_n W_n)^T$.

Apply SVD on S' and the resulted matrices are U_W, S_W and V_W, i.e. $S' = U_W S_W V_W^T$, where U_W, V_W are orthogonal matrices and S_W is a diagonal matrix with embedded watermark. Now Watermarked image, F_W is obtained by multiplying three matrices U, S_W and V^T, i.e. $F_W = U S_W V^T$. From the attacked versions of the watermarked image F_W*, a watermark is extracted as follows. Apply SVD on possibly modified watermarked image resulting three matrices U*, S_W* and V^{*T}.

$$F_W^* = U^* S_W^* V^{*T}$$

And then calculate

$$D^* = U_W S_W^* V_W^T$$

The extracted watermark W* is

$$W^* = (1/\alpha)(D^* - S).$$

The normalized cross correlation between inserted and extracted watermark (NC (W, W*)) is calculated . Then fitness for the watermarked image is calculated as a function of imperceptibility and robustness by using Tabu search as explained under Tabu-

THE IIOAB JOURNAL
ISSN: 0976-3104

search. For the initial random set of scaling factors, original image is watermarked and the fitness value is calculated for the attacked watermarked images. The set of scaling factors with minimum fitness value is utilized for generating candidate solutions as explained under Tabu-search. The candidate solution having minimum fitness value is selected for generating next set of scaling factors. If the Candidate solution already exists in Tabu list, pick the next candidate solution having minimum fitness. If the termination condition is met, then stop the operation. Otherwise, the new set of the scaling factor is used to generate the candidate solutions until the termination criteria is met.

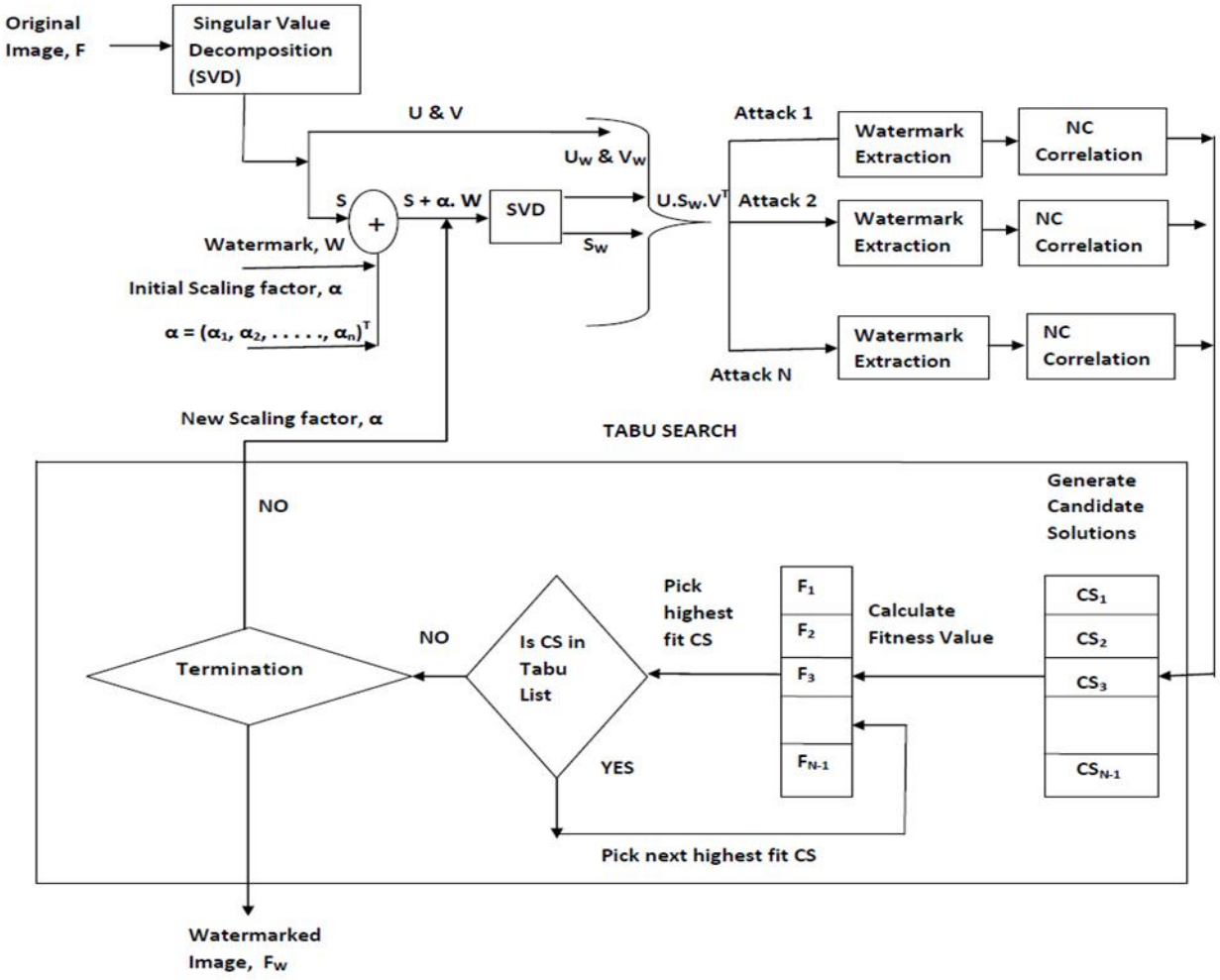

Fig: 1. Block diagram for the proposed watermarking algorithm

Block-wise SVD watermarking

In order to capture the local properties of image in watermarking, Block-Wise SVD can be considered.
Block-Wise SVD watermarking algorithm is explained in the **Fig: 2.**
The Original image F is of size M x N and Watermark image W is of size a x b.

1) Divide F into blocks of size 8 x 8, then there will be M/8 x N/8 blocks.

2) A watermark W is linearized in row major fashion, say W' is of size 1 x ab, W'(i) is the ith value of W, using row major scheme.

3) F has M/8 x N/8 blocks, linearize the blocks in row major fashion as B (i), $1 \leq i \leq$ M/8 x N/8 .

THE IIOAB JOURNAL
ISSN: 0976-3104

Case- I: Considering highest singular value in each 8 x 8 block for watermarking

In this case, highest singular value in each 8 x 8 block is considered for watermarking as it has high energy concentration.

1) Calculate $T = \frac{ab}{(\frac{M}{8})^2}$, where ab is number of linearized watermark coefficients, in order to compute how many watermark coefficients needs to be inserted in each of the 8 x 8 blocks. .

2) If T ≤ 1, then the size of the linearized watermark W' is less than the number of blocks. So,W'(i) is inserted into B(i), 1 ≤ i ≤ ab .

3) If T > 1, we can insert more than one watermark coefficient in each 8 x 8 block. So, $\lceil T \rceil$ number of watermark coefficients need to be insertyed in each 8 x 8 block.

4) The strength of the watermark, W'(i) ,1 ≤ i ≤ ab, is modified by set of scaling factors α = (αi) ,1 ≤ i ≤ ab.

5) The SVD is performed for each 8 x 8 block individually and arranged linearly in row major order.

6) The first singular value of the SVD of each block is modified by adding watermark coefficients with some strength i.e. scaling.

7) This set of scaling factors is determined by Tabu search algorithm. This technique is robust to cropping and average filtering attacks.

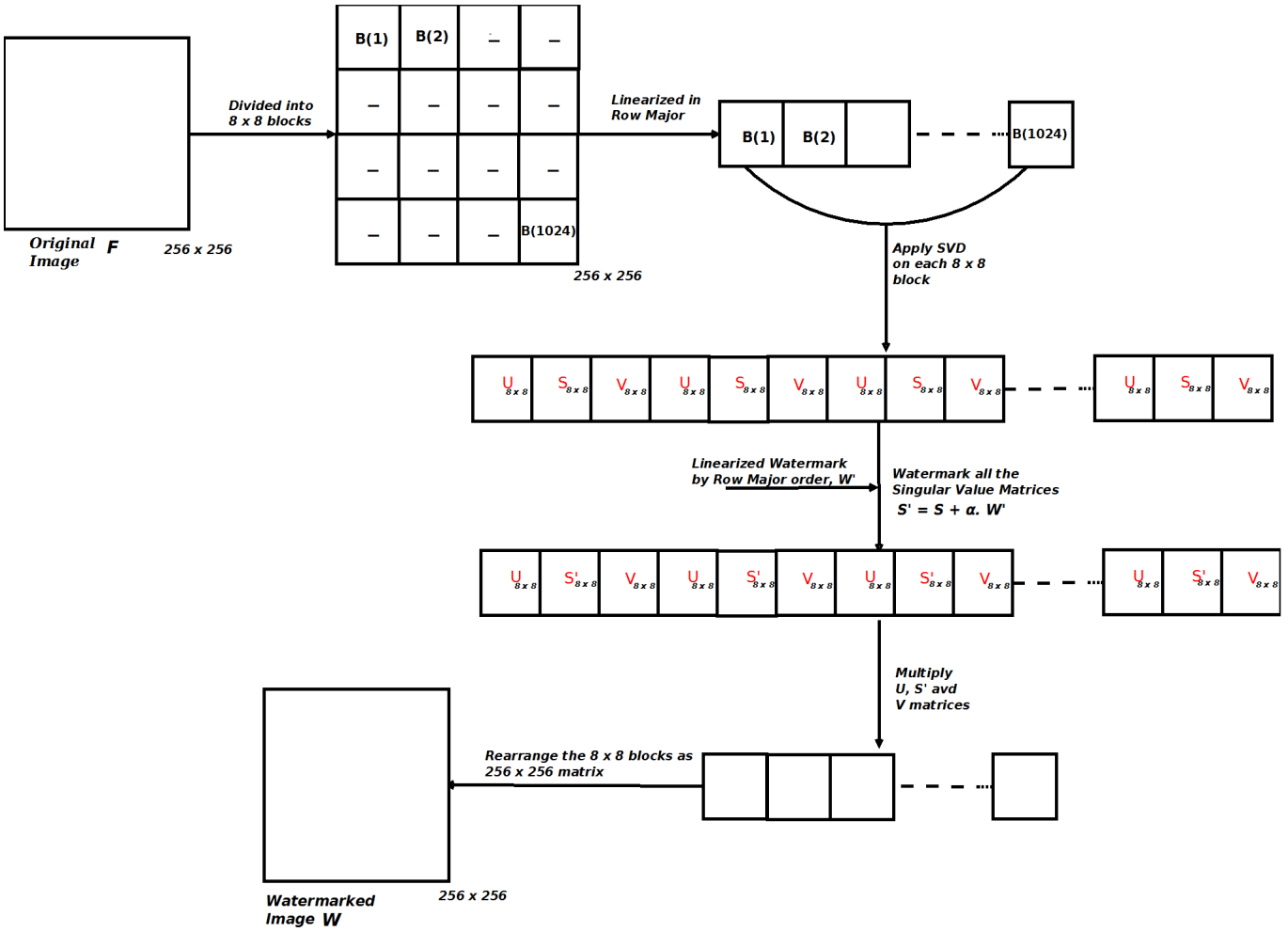

Fig: 2. Block diagram for the block-wise SVD watermarking algorithm

THE IIOAB JOURNAL
ISSN: 0976-3104

Block-wise SVD watermarking

Case II: Considering all the singular values for watermarking

In this case, all the singular values of each 8 x 8 block are considered for watermarking. Details are given below:

1) For example, the size of an original image F is 256 x 256 and the size of watermark image W is 32 x 32.

2) The original image is divided into 8 x 8 blocks, i.e. 1024 blocks of size 8 x 8 are available.

3) These blocks are organized linearly using row major fashion, i.e. B(i), $1 \leq i \leq 1024$, where i corresponds to one 8 x 8 block.

4) The watermark is also linearized in row major order, i.e. W'(i), $1 \leq i \leq 1024$.

5) If SVD is performed on B, then 8192 singular values will be available. In order to watermark all the singular values, the linearized watermark W' is expanded by a factor of 8 (8 copies of W').

6) The expanded watermark ,We (8 copies of W' that is of size 1 x 8192) is used for watermarking. Here for every 8 x 8 block two orthogonal matrices U & V and one diagonal matrix S will be available after performing SVD.

7) For 1024 blocks, U and V matrices are stored in a linear fashion.

8)The number of singular values available is 8192 and the size of expanded watermark, We is 1x 8192. So, all the singular values of diagonal matrix S are watermarked in order to incorporate watermark in all 8 x 8 blocks and the modified Singular value matrix is S'. For Case II, the watermark W' needs to be replaced by We, in **Figure-2.**

9) The strength of the watermark is modified by a set of scale factors $\alpha = (\alpha i)$, where $1 \leq i \leq 8192$. This set of scaling factors is determined by Tabu search algorithm. Then Watermarked image is obtained by multiplying all three matrices U, S' and VT and rearranging to the image of size 256 x 256 as shown in **Figure-2**.

RESULTS

The proposed watermarking scheme has been verified with the following attacks: Cropping, Rotation, Gaussian Noise, Average Filtering, Histogram equalization and JPEG compression. The experimental results have been compared with the results presented in [20] as shown in **Table−1**. For doing comparison between the inserted and extracted watermarks, 2D normalized correlation (NC) was used. If NC is closer to 1 then extracted watermark is closer to the inserted watermark. By considering multiple scaling factors for embedding the watermark we can achieve good improvement on robustness. More the strength of the scaling factor, better the robustness. On the dataset given in [54], the proposed technique is implemented and the average NC values are listed in **Table−2**. The original image, watermark and the extracted watermarks after attacks have been shown in **Figure− 3.**

The watermarked image is cropped for different rows and columns and the NC values are listed in **[Table−3]**. JPEG compression with different quality factors have been performed on the watermarked image and the NC between the inserted and extracted watermark is calculated and listed in **[Table−4]**. NC values for different rotated versions of the watermarked image is computed and compared with the algorithm presented in [20]. The cropped, average filtered and rotated version of the watermarked image is as shown in **Figure− 4.**

Table: 1. NC values of the extracted watermarks from different attacks for the image given in Fig: 2 (a)

Attack	NC for proposed	NC for SVD+GA[20]
Crop	0.9996	0.9996
Rotation	0.9932	0.9701
Gaussian Noise	0.9089	0.9069
Average Filtering	0.9804	0.9795
Histogram Equalization	0.9314	0.9286
JPEG Compression	0.9535	0.9415

THE IIOAB JOURNAL
ISSN: 0976-3104

Table: 2. Average NC values of the extracted watermarks from different attacks on images given in [54]

Attack	NC for proposed	NC for SVD+GA[20]
Crop	1(with 5 decimations)	0.99952
Rotation	0.994	0.9939
Gaussian Noise	0.885	0.888
Average Filtering	0.983	0.9817
Histogram Equalization	0.903	0.904
JPEG Compression	0.957	0.953

Table: 3. NC values of watermarked image for different cropped versions for image given in Fig: 3 (a)

Number of Rows Cropped (Out of 256)	Number of columns cropped (Out of 256)	NC for proposed	NC for SVD+GA[20]
0	First 20 and last 6 columns	0.9996	0.9999
0	First 50 and last 6	0.9978	0.999
0	First 50 and last 56	0.9926	0.9937
0	First 20 and last 256	0.9956	0.9935
First 50	First 50	0.9911	0.999
First 100	First 50	0.9913	0.994
First 150	First 150	0.9743	0.9736
First 100	First 100	0.9895	0.9887

Table: 4. NC values of JPEG compression for different quality factors for image given in Fig: 2 (a)

JPEG quality factor	NC for proposed	NC for SVD+GA[20]
50	0.9799	0.9798
75	0.9856	0.9851
90	0.9881	0.9872
95	0.9886	0.9876

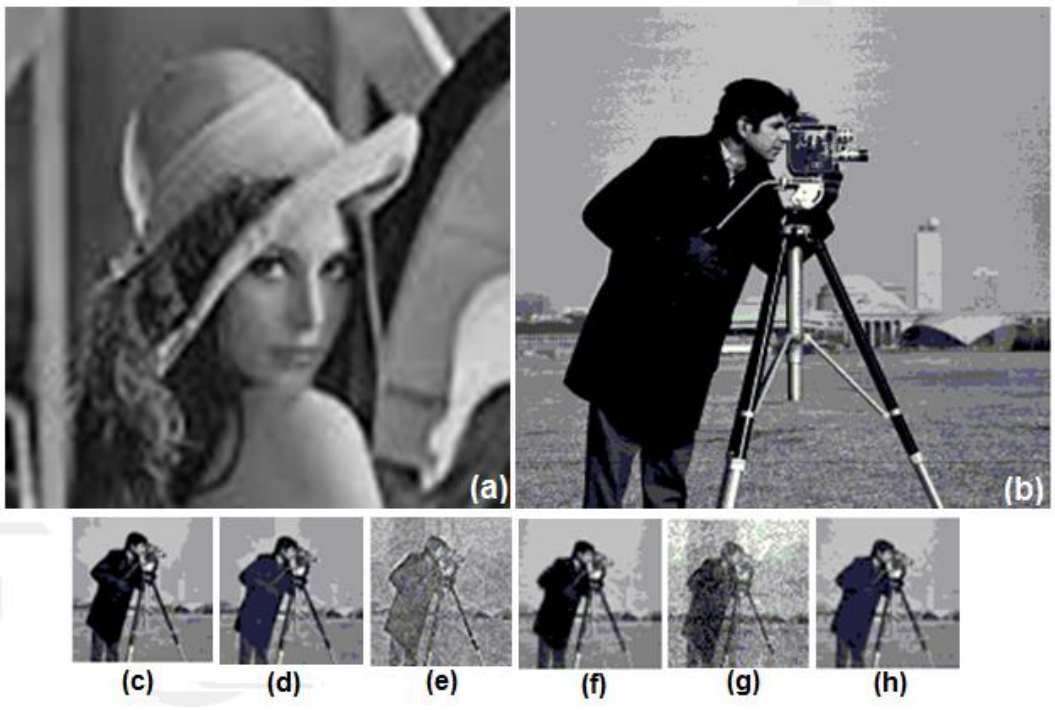

Fig: 3. (a) Original image, **(b)** watermark, **(c)** Extracted watermarks after cropping, **(d)** Rotation, **(e)** Gaussian noise, **(f)** Average filtering, **(g)** Histogram equalization and **(h)** JPEG compression attacks respectively

THE IIOAB JOURNAL
ISSN: 0976-3104

Table: 5. NC values of Watermarked image for rotation of the image given in Fig: 3 (c)

Rotation (in degrees)	NC for proposed	NC for SVD+GA[20]
-45	0.9785	0.9775
-15	0.9902	0.9901
-5	0.9985	0.9985
-2	0.9995	0.9996
2	0.9989	0.9988
5	0.9957	0.9954
15	0.9851	0.9851
45	0.9785	0.9775

Fig: 4. (a) Cropped, **(b)** Average filtered and **(c)** Rotated version of watermarked image respectively

DISCUSSION

In order to evaluate the performance of the proposed watermarking scheme, experiments have been conducted on all the images from the dataset [54]. The robustness of the proposed scheme have been evaluated with different attacks such as rotation, cropping, JPEG compression, Histogram equalization, Average filtering and Gaussian noise and compared with the algorithm presented in [20]. The strength of the watermark will modify the quality of the singular values of the image. So, instead of maintaining constant scaling factor for all the singular values, multiple scaling factors are used that are optimal for each singular value of the image. The proposed Watermarking algorithm uses Tabu Search for finding optimal scaling factors with anti-cycling memory, which will avoid the search of generating a set of scaling factors that has been already generated in the previous steps. So, at every step, a new set of scaling factor, better than the previous set will be generated, providing better robustness and imperceptibility of the watermarking algorithm.

CONCLUSIONS

A digital image watermarking scheme based on SVD and Tabu search has been proposed in this paper. Multiple scaling factors are used to embed the watermark in the diagonal matrix instead of one constant value. Tabu search is used to optimize multiple scaling factors for different singular values of the diagonal matrix to embed the watermark. The proposed method performs successfully during the attacks and the watermark can be extracted with very less degradation. During the attacks, the correlation between the extracted and inserted watermark is closer to 1 (means similar) and it performs better than the other similar works. It is observed that the proposed method is more robust compared to the algorithm that used Genetic algorithm for finding optimal scaling factors.

.

CONFLICT OF INTEREST
Authors declare no conflict of interest.

ACKNOWLEDGEMENT
None.

FINANCIAL DISCLOSURE
No financial support was received to carry out this project.

THE IIOAB JOURNAL
ISSN: 0976-3104

REFERENCES

[1] Rafael C Gonzalez, Richard E Woods, Digital image processing, Third edition, Pearson Publishers, 842−852.

[2] Potdar, Vidyasagar M., Song Han, and Elizabeth Chang [2005] "A survey of digital image watermarking techniques" in IEEE 3rd IEEE International Conference on Industrial Informatics, 709−716.

[3] Cox, Ingemar J, Joe Kilian, F Thomson Leighton, and Talal Shamoon.[1997] Secure spread spectrum watermarking for multimedia, IEEE Transactions on Image Processing, 6(12): 1673−1687.

[4] Cao JG, James E Fowler, and Nicholas H Youman, [2001] An image-adaptive watermark based on a redundant wavelet transform, in the proceedings of *IEEE International Conference on Image Processing*, 2: 277−280.

[5] Joshi, Vaibhav and MilindRane. [2014] Digital Watermarking using LSB replacement with Secret key insertion Technique.

[6] Xia, Xiang-Genm Charles G Boncelet, and Gonzalo R Arce. [1997] A Multi resolution Watermark for digital Images, in the proceedings *of IEEE International Conference on Image Processing*, 1: 548551.

[7] Liu Ruizhen, and Tieniu Tan. [2002] "An SVD based Watermarking Scheme for Protecting rightful ownership, *IEEE Transactions on Multimedia* 4(1): 121−128.

[8] Wang Shuo-zhong. [2000] Watermarking based on principal component analysis, *Journal of Shanghai University (English Edition)* 4(1): 22−26.

[9] Cox Ingemar J, and Matt L Miller. [1997] Review of Watermarking and the importance of perceptual Modeling, in *Electronic Imaging, International Society for Optics and Photonics*, 92−99.

[10] Majumder Swanirbhar, Kharibam Jilenkumari Devi, and Subir Kumar Sarkar, [2013] Singular Value Decomposition and Wavelet based IRIS biometric Watermarking, *IET Biometrics*, 2(1): 21−27.

[11] Kaewkamnerd N, and K R Rao. [2000] Wavelet based Image Adaptive Watermarking Scheme, *Electronics Letters*, 36(4): 312−313.

[12] Kundur D, Hatzinakos D. [1998] Digital Watermarking using Multiresolution Wavelet Decomposition, Proc. IEEE Int. Conf. On Acoustics, Speech and Signal Processing, Seattle, Washington, 5: 2969−2972.

[13] Zhu W, Xiong Z, and Zhang YQ. [1999] Multiresolution Watermarking for Images and Video, in *IEEE Trans. on circuit and System for Video Technology*, 9(4): 545−550.

[14] Kaewkamnerd N, Rao KR. [2005] Multiresolution based image adaptive watermarking scheme, in EUSIPCO, Tampere, Finland, (Available online www.ee.uta.edu/dip/paperfEUSIPCO water.pdf).

[15] Kaewkamnerd N, Rao KR. [2000] Wavelet based image adaptive watermarking scheme in *IET Electronics Letters*, 36(4): 312−313.

[16] Xie L, Boncelet, G, Acre, GR. [1998] Wavelet transform based watermarking for digital images, *in Optics Express*, 3(12): 497−511.

[17] Hsu CT, Wu JL. [1998] Multiresolution Watermarking for Digital Images, in IEEE Transactions on Circuits and Systems - II: Analog and Digital Signal Processing, 45(8): 1097−1101.

[18] Raval MS, Rege PP. [2003] Discrete wavelet transform based multiple watermarking scheme, Conference on Convergent Technologies for Asia-Pacific Region, TENCON 2003, 3: 935−938.

[19] Kundur D, Hatzinakos D. [1998] Digital Watermarking using Multiresolution Wavelet Decomposition, in Proc. *IEEE Int. Conf On Acoustics, Speech and Signal Processing, Seattle*, Washington, 5: 2969−2972.

[20] Lai, Chih-Chin.. [2011] A digital watermarking scheme based on singular value decomposition and tiny genetic algorithm, *Digital Signal Processing*, 21(4):522−527.

[21] Ayesha Sk, VM Manikandan, and V Masilamani. [2015] A Combined SVD-DWT Watermarking Scheme with Multi-level compression Using Sampling and Quantization on DCT Followed by PCA, In Proceedings of the 3rd International Conference on Frontiers of Intelligent Computing: Theory and Applications (FICTA) 2014, *Springer International Publishing*, 141−149.

[22] Lee C, Lee H. [2005] Geometric attack resistant watermarking in wavelet transform domain, in Optics Express 13(4): 1307−1321.

[23] Zhu W, Xiong Z, Zhang Y-Q. [1999] Multiresolution Watermarking for Images and Video, in *IEEE Trans*. on circuit and System for Video Technology, 9(4): 545−550.

[24] Tao B, Dickinson B. [1997] Adaptive Watermarking in DCT Domain, in Proc. *IEEE International Conference* on Acoustics, *Speech, and Signal Processing*, 4: 1985−2988.

[25] Fotopoulos V, Skodras AN. [2000] A Subband DCT Approach to Image Waternarking, in Proceedings of *X European Signal Processing Conference*, Tampere, Finland.

[26] Choi Y, Aizawa K. [2002] Digital Watermarking Technique using Block Correlation of DCT Co*efficients, in* Electronics and Communications, Japan, Part 2 85(9): 23−31.

[27] Suhail M, A Obaidat, MS. [2003] Digital Waternarking Based DCT and JPEG Model, in *IEEE Transactions on Instrumentation and Measurement*, 52(5): 1640−1647.

[28] Golikeri A, Nasiopoulos P. [2005] A Robust DCT Energy Based Watermarking scheme for Images, *Journal of proceedings of IEEE* (Available Online: www.ece.ubc.ca/~adarshg/DCT_Watermark.pdf).

[29] Ganic Enir, and Ahmet M Eskicioglu, [2004] Robust DWT-SVD domain image watermarking: embedding data in all frequencies, in proceedings of the *ACM Workshop on Multimedia and Security*, 166−174.

[30] Zheng Dong, Jiying Zhao, Abdulmotaleb El Saddik, [2003] RST – Invariant digital Image watermarking based on log-polar mapping and phase correlation, *IEEE Transactions on Circuits and Systems for Video Technology*, 13(8): 753−765.

[31] Ho Anthony TS, Jun Shen and Soon H Tan. [2003] Robust Digital Image-in-image watermarking algorithm using the fast Hardamard Transform, in International Symposium on Optical Science and Technology, *International Society for Optics and Photonics*,76−85.

[32] Zheng, Peijia and Jiwu Hauns, [2013] Walsh Hadamard Transform in the homomorphic encrypted domain and its applications in Image watermarking, in Information Hiding, *Springer Berlin Heidelberg*, 240 – 254.

THE IIOAB JOURNAL
ISSN: 0976-3104

[33] Mohan B Chandra, and S Srinivas Kumar [2008] A Robust Image Watermarking Scheme using Singular Value Decomposition, *Journal of Multimedia* 3(1): 7−15.

[34] Bao Paul, Xiaohu Ma. [2005] Image Adaptive Watermarking using Wavelet domain Singular Value Decomposition, *IEEE Transactions on Circuits and Systems for Video Technology*, 15(1): 96 − 102.

[35] Cox Ingemar J, Mathew L Miller, Jeffrey Adam Bloom and Chris Honsinger, [2002] Digital Watermarking, Vol. 53, San Francisco, Morgan Kaufmann.

[36] Hao Yin, QiuFeng Lin Chuang, and Ding Rong. [2005] A Survey of Digital Watermarking" *Journal of Computer Research and Developmen*t, 42(7): 1093−1099.

[37] Zhao Y, Campisi, P, Kundur D. [2004] Dual Domain Watermarking for Authentication and Compression of Cultural Heritage Images, in *IEEE Transactions on linage Processing*, 13(3): 430−448.

[38] Tao P , Eskicioglu, AM. [2004] A Robust Multiple Watermarking Scheme in the Discrete Wavelet Transform Domain, in Symposium on Internet Multimedia Management Systems V, Philadelphia, 133−144.

[39] Ganic E, Eskicioglu, AM. [2004] Robust digital watermarking: Robust DWT-SVD domain image waternarking: embedding data in all frequencie", Proceedings of the multimedia and security workshop on Multimedia and Security, 166 – 174.

[40] Pereira S, Pun T. [2000] Robust Template Matching for Affine Resistant Image Watermarks, in *IEEE Transactions on Image Processing*, 9(6): 1123−1129.

[41] Solachidis V, Pitas I. [2001] "Circularly Symmetric Watermark Embedding in 2-D DFT Domain, in IEEE Transactions on Image Processing, 10(11): 1741−1753.

[42] Ganic E, Dexter SD, Eskiciogl, AM. [2005] Embedding Multiple Watermarks in the DFT Domain Using Low and High Frequency Bands, IS&T/SPIE's 17th Annual Symposiun on Electronic lmaging, Security, Steganography, and Watermarking of Multitnedia Contents VII Conference, San Jose, CA.

[43] Ruanaidh JJK O, Dowling WJ, Borland FM. [1996] Phase watermarking of digital images, in Proc. *IEEE Int. Conf: Image Processing*, 239−242.

[44] Lin C-Y, Wu M, Bloom JA, Cox U, Mille, ML &Lui, YM. [2001] Rotation, Scale and Translation Resilient Watermarking for Images, *IEEE Transactions on Image Processing*, 10(5): 767−782.

[45] Gilani AM. Skodras AN. [2001] Watermarking by Multi-resolution Hadamard Transform, in Proceedings *Electronic Imaging & Visual Arts (EVA 2001*), 73−77.

[46] Falkowski BJ, Lim LS. [2000] Image Waternarking Using Hadamard Transforms", in IEE Electronics Letters, United Kingdom, 36(3): 211−213.

[47] Noore A. [2003] An improved digital watermarking technique for protecting JPEG images in *IEEE International Conference on Consumer Electronics*, Morgantown, WV, USA, 222−223.

[48] Podilchuk Christine I, and WenjunZeng. [1998] Image-adaptive watermarking using visual models, Selected Areas in Communications*, IEEE Journal*, 4;. 525−539.

[49] Bhatnagar, Gaurav, and Balasubramanian Raman. [2009] Robust watermarking in multiresolution Walsh-Hadamard Transform, In *IEEE International Conference on Advance Computin*g, 894−899.

[50] Marjuni Aris, RajasvaranLogeswaran, and MF Ahmad Fauzi. [2010] An image watermarking scheme based on FWHT-DCT", In *IEEE International Conference on Networking and Information Technology (ICNIT)*, 289−293.

[51] Tsai, Hung-Hsu, and Shih-Che Lo. [2014] JND-based watermark embedding and GA-based watermark extraction with fuzzy inference system for image verification, *Informatica* 25(1) 113−137.

[52] Boland FRANCIS MORGAN, JJK O Ruanaidh, and C Dautzenberg. [1995] Watermarking digital images for copyright protection", In Fifth IET International Conference on Image Processing and its Applications, 326−330.

[53] Basso, Alessandro, Francesco Bergadano, Davide Cavagnino, Victor Pomponiu, and AnnamariaVernone. [2009] A novel block-based watermarking scheme using the SVD transform, *Algorithms* 2(1):46−75.

[54] http://lear.inrialpes.fr/jegou/data.php#copydays (May 2014).

[55] http://sipi.usc.edu/database/

ABOUT AUTHORS

Ayesha Shaik *received the B.Tech degree in Electronics and Communications Engineering in 2008 and M.Tech degree in VLSI design in 2013 from JNTU Anantapur. Currently, she is a research scholar in the Department of Computer Engineering, Indian Institute of Information Technology, Design and Manufacturing (IIITD&M) Kancheepuram. Her research interests include Digital Image Processing, Watermarking, and Hardware implementation of image security algorithms.*

Masilamani V. *is currently Assistant Professor in the Indian Institute of Information Technology,Design and Manufacturing, Kancheepuram, India. He is currently faculty in the department of Computer Science. He received his M.Tech degree from Indian Institute of Technology, Kharagpur, India. He completed his Ph.D. from Indian Institute of Technology, Madras, India. His research interest includes Image Processing and theoretical computer science. He has teaching experience of 10 years and research experience of 8 years. He has a number of international journal and conference publications.*

ISSN: 0976-3104
REGULAR ISSUE
Hui

THE IIOAB JOURNAL

ARTICLE OPEN ACCESS

FULMINANT THROMBOTIC THROMBOCYTOPENIC PURPURA IN CHRONIC HEPATITIS B VIRUS INFECTION WITH SEVERE FIBROSIS

Chee-Kin Hui[1,2]

[1]*Centre For Alimentary Studies, Hong Kong SAR, CHINA*
[2]*Quality Healthcare Medical Services, Hong Kong SAR, CHINA*

ABSTRACT

A 57-year old man with chronic hepatitis B virus (HBV) infection, mild thrombocytopenia and mild hemolytic anaemia was started on Entecavir for treatment of chronic HBV. He was readmitted for fever, confusion, severe hemolytic anaemia, and, severe thrombocytopenia eight weeks later. A disintegrin and metalloproteinase with a thrombospondin type-1 motifs 13 (ADAMTS13) activity and antigen were severely low with a positive ADAMTS13 autoantibody. His serum HBV DNA at this stage was less than 20 IU/ml. He was diagnosed with fulminant TTP. In conclusion, fulminant TTP can occur in those with chronic HBV upon immune recovery induced by potent anti-HBV therapy.
.

Received on: 4th-June-2015
Revised on: 14th-June-2015
Accepted on: 15th-June-2015
Published on: 22nd-July-2015

KEY WORDS

Thrombotic thrombocytopenic purpura; hepatitis B virus; ADAMTS13; human immunodeficiency virus; von Willebrand factor; Computerized tomography

***Corresponding author:** **Email:** bckhui@gmail.com; **Tel.:** +852 2723 1183; **Fax:** +852 2723 6620

INTRODUCTION

Thrombotic thrombocytopenic purpura (TTP) is an uncommon disease. It is characterized by microangiopathic hemolytic anaemia, thrombocytopenia, neurologic symptoms, renal involvement and fever. TTP has been reported to be associated with viral infections such as the human immunodeficiency virus (HIV) [1], influenza A [2], and, also in chronic hepatitis C virus infected patients on interferon treatment [3]. Here, is a case of chronic hepatitis B virus (HBV) infection who developed fulminant TTP after viral suppression was achieved with Entecavir.

CASE REOPORT

A 57 year old Chinese gentleman presented with a 3-month history of progressive malaise. He was found to have deranged liver function with albumin 42 g/dl (normal range 35-50), alanine aminotransaminase 284 IU/L (normal range 6-53), aspartate aminotransaminase 189 IU/L (normal range 13-33), total serum bilirubin 30 µmol/L (normal range 3-22), and, direct bilirubin 3 umol/L (normal range <3) with indirect bilirubin 27 umol/L (normal range <14).

Complete blood count and coagulation profile were as follows: haemoglobin 11.1 gm/dl (normal range 13.0-17.0), platelets 104 K/ul (normal range 140-400), prothrombin time (PT) 13.70 seconds (normal range 10.10-12.60), International Normalized Ratio 1.18 (normal range 0.90-1.10), activated partial thromboplastin time 33.4 seconds (normal range 24.4-32.0).

He was found to be hepatitis B surface antigen positive, hepatitis B e antigen negative with a positive hepatitis B e antibody. The serum HBV DNA was 8.75 X 10^5 IU/ml (COBAS TaqMan HBV assay, Roche Diagnostics, Branchburg, New Jersey, USA). Computerized tomography (CT) of the whole abdomen showed a normal sized liver but with lobulated contour and heterogenous attenuation suggestive of liver cirrhosis. The size of the spleen was normal on CT scan. Fibroscan of the liver was 11.4 kPa.

THE IIOAB JOURNAL
ISSN: 0976-3104

A disintegrin and metalloproteinase with a thrombospondin type-1 motifs 13 (ADAMTS13) activity, performed with a commercially available assay based on the fluorescence resonance energy transfer (FRET) method using an artificial von Willebrand factor (vWF) fragment, was 35% (normal range 70-160). ADAMTS13 (vWF cleaving protease) antigen level, performed by a commercial ELISA assay in accordance with the manufacturer instructions, was 130.5 ng/ml (normal range 253-2238). However, ADAMTS13 autoantibody, performed by a commercial ELISA assay, was negative. His blood film was not reviewed at this stage.

He was started on Entecavir 0.5 mg daily. His serum alanine aminotransaminase and HBV DNA after commencement of Entecavir are shown in **Table-1.**

Table: 1. Table showing serial blood results.

Week on Entecavir	0	1	4	8	16
Serum HBV DNA (Log10 IU/ml)	5.94	4.23	1.30	1.30	1.30
Serum Alanine aminotransaminase (IU/L)	286	55	43	22	20
Haemoglobin (g/dl)	11.1	11.6	12	8.6	10
Platelet (K/ul)	104	100	101	21	147
Total Bilirubin (umol/l)	30			53.6	22.6
Direct Bilirubin (umol/l)	3			9	7.6
Indirect Bilirubin (umol/l)	27			42	15
Lactate Dehydrogenase (U/L)	514			966	383
Prothrombin Time (seconds)	13.7			19.7	11.2
ADAMTS13 Activity (%)	35			3	62
ADAMTS13 Antigen (ng/ml)	130.5			48	234
ADAMTS13 Autoantibody	Negative			Positive	Positive
Fibroscan (kPa)	11.4			11.0	11.6

Eight weeks after commencement of Entecavir, he was readmitted for fever and confusion. Physical examination was unremarkable with no flapping tremor or focal neurological sign.

His blood investigation on readmission showed haemoglobin 8.6 gm/dl, platelets 21 K/ul, serum alanine aminotransaminase was normal, serum total bilirubin 53.6 umol/L, direct bilirubin 9 umol/L with indirect bilirubin 42 umol/L, serum HBV DNA < 20 IU/ml, serum lactate dehydrogenase 966 IU/L (normal range 197-401), prothrombin time 19.70 seconds, activated partial thromboplastin time 35.0 seconds, and, a low plasma haptoglobulin level 4 mg/dl (normal range 20-190).

Blood film review showed considerable variation in red cell size and shape. Elliptocytes and a few target cells were found in association with fragments **[Figure-1]**. Platelets were reduced and large forms were frequent.

His ADAMTS13 activity had decreased to 3% with ADAMTS13 antigen reduced to 48 ng/ml. He had developed a positive ADAMTS13 autoantibody as well. Bone marrow aspirate showed megakaryocytic hyperplasia with left shifted granulocytic series and reactive changes.

Autoimmune antibodies, Coombs test, cytomegalovirus pp65, cytomegalovirus immunoglobulin (Ig) M and, HIV I and II antibody were all negative. Arterial ammonia, urine for routine microscopy and serum creatinine were all normal.

He was diagnosed with fulminant TTP and remission was achieved with fresh frozen plasma infusion, Rituximab and corticosteroid. His platelet count, bilirubin, haemoglobin, reticulocyte count, ADAMTS13 activity, ADAMTS13 antigen and ADAMTS13 autoantibody 8 weeks after treatment for fulminant TTP was started (16 weeks after commencement of Entecavir) are shown in **Table-1**.

THE IIOAB JOURNAL
ISSN: 0976-3104

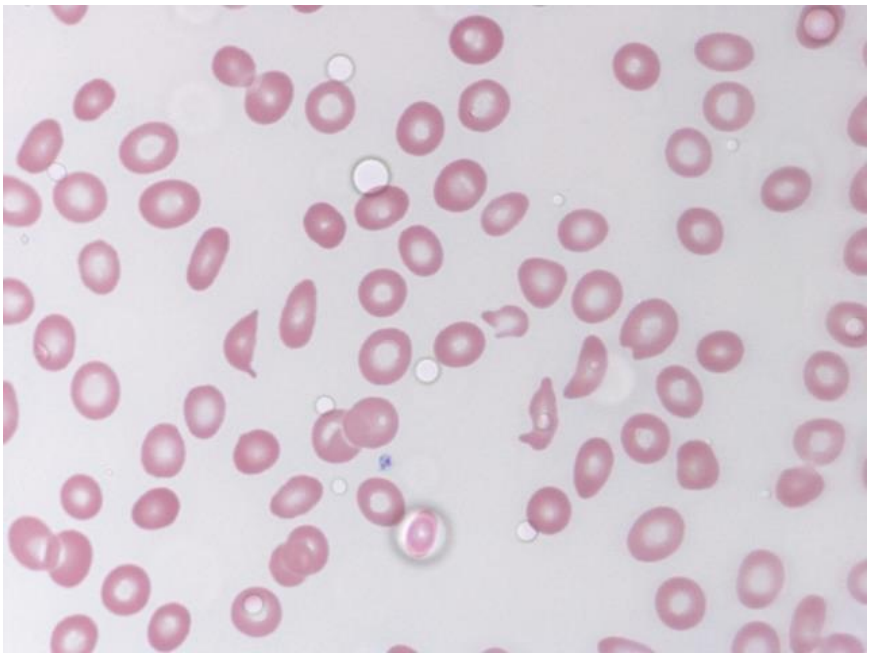

Fig: 1. Slide showing fragmented red blood cells

DISCUSSION

Most of the reported cases of HIV infection associated TTP were characterized by fulminant syndrome [1]. Veenstra et. al. were the first to report low-grade TTP associated with HIV-infection [4]. These low-grade TTP would usually occur late in the natural history of HIV-related disorders [4].

Here, is the first reported case of TTP associated with chronic HBV infection. Retrospectively, he may have been suffering from low-grade TTP at the time of presentation. This is because he already had thrombocytopenia, and, anaemia with raised indirect serum bilirubin and PT [**Table-1**] suggestive hemolysis.

However, as the ADAMTS13 activity was only mildly to moderately reduced along with a negative ADAMTS13 autoantibody, it was presumed to be a secondary reduction due to his acute reactivation of chronic HBV infection and severe liver fibrosis, based on his liver stiffness score on Fibroscan [5,6]. Whether this low-grade TTP would occur late in the natural history of chronic HBV infection, when the chronic HBV has been complicated by severe liver fibrosis or liver cirrhosis similar to that observed in HIV-related disorders, is uncertain [1].

He developed fulminant TTP after complete viral suppression was achieved. This is probably because rapid viral suppression by potent anti-HBV therapy has been shown to be associated with immune recovery or immune reconstitution [7].

This immune recovery can result in an immune reconstitution inflammatory syndrome similar to that most commonly observed in HIV infection [8]. The pathogenesis of immune reconstitution inflammatory syndrome has been postulated to be due to a combination of thymic-independent homeostatic peripheral expansion, immune dysregulation between effector and regulatory T-cells, increased inflammatory cytokines and dysregulated dendritic cells [8].

The immune recovery achieved with potent anti-HBV therapy may have resulted in neutralizing IgG-autoantibodies being produced [7]. This autoantibody would inhibit vWF-cleaving protease activity, thus impairing the ability of ADAMTS13 to cleave ultra-large vWF in the plasma and on the surface of endothelial cells. This is similar to the clinical picture of acute TTP observed in acquired idiopathic TTP.

THE IIOAB JOURNAL
ISSN: 0976-3104

These IgG antibodies that inhibit ADAMTS13 activity have been reported in 48% to 80% of those with recurrent or acute TTP [9]. This suggests that their presence have a role in recurrent or acute TTP.

This case report suggests that fulminant TTP may occur in chronic HBV infection with severe fibrosis. When immune recovery was achieved with potent anti-HBV therapy, it may have triggered the production of anti-ADAMTS13 antibodies. The anti-ADAMTS13 antibodies subsequently resulted in an episode of fulminant TTP.

CONCLUSION

In conclusion, chronic HBV infection with severe fibrosis may be associated with fulminant TTP. This calls for a high index of suspicion and vigilance on the possibility of this association. Therefore, TTP should be considered as a differential in a chronic HBV infected patient with thrombocytopenia and anaemia. This fulminant TTP is associated with severe ADAMTS13 deficiency and antibody formation.

CONFLICT OF INTEREST

Authors declare no conflict of interest.

ACKNOWLEDGEMENT

None.

FINANCIAL DISCLOSURE

No financial support was received to carry out this project.

REFERENCES

[1] Nosari AM, Landonio G, Caggese L, Cattaneo D, Muti G, Volonterio A. [1994] Thrombotic thrombocytopenic purpura associated with HIV infection: report of two cases. *Hematologica* 79: 280−282.

[2] Kosugi N, Tsurutani Y, Isonishi A, Hori Y, Matsumoto M, Fujimura Y. [2010] Influenza A infection triggers thrombotic thrombocytopenic purpura by producing the Anti-ADAMTS13 IgG *inhibitor. Inter Med* 49: 689−693.

[3] Deutsch M, Manesis EK, Hadziyannis E, Vassilopoulos D, Archimandritis AJ. [2007] Thrombotic thrombocytopenic purpura with fatal outcome in a patient with chronic hepatitis C treated with pegylated interferon-a/2b. *Scan J Gastroenterol* 42: 408−409.

[4] Veenstra J, Van der Lelie J, Mulder JW, Reiss P. [1993] Low-grade thrombotic thrombocytopenic purpura associated with HIV-1 infection. *Br J Haematol* 83: 346−347.

[5] Castera L, Vergniol J, Foucher J, et al. [2005] Prospective comparison of transient elastography, Fibrotest, APRI, and liver biopsy for the assessment of fibrosis in chronic hepatitis *C. Gastroenterology* 128: 343−350.

[6] Hui CK, Leung N, Shek TW, et. Al. [2007] Sustained disease remission after spontaneous HBeAg seroconversion is associated with reduction in fibrosis progression in chronic hepatitis B Chinese patients. *Hepatology* 46: 690−698.

[7] Hui CK, Zhang HY, Bowden S, et. A.l [2007] 96 weeks combination of adefovir dipivoxil plus emtricitabine versus adefovir dipivoxil monotherapy in the treatment of chronic hepatitis B. *J Hepatol* 48: 714−720.

[8] Drake WP, Byrd VM, Olsen NJ. [2003] Reactivation of systemic lupus erythematosus after initiation of highly active antiretroviral therapy for acquired immunodeficiency syndrome. *J Clin Rheumatol 9*: 176−180.

[9] Kremer Hovinga JA, Lammle B. [2012] Role of ADAMTS13 in pathogenesis, diagnosis and treatment of thrombotic thrombocytopenic purpura. *Hematology Am Soc Hematol Educ Program* 610−616.

ISSN: 0976-3104
REGULAR ISSUE
Singh et al.

THE IIOAB JOURNAL

RESEARCH ARTICLE OPEN ACCESS

THE EFFECT OF FINISHING AND POLISHING PROCEDURES ON THE SURFACE ROUGHNESS OF COMPOSITE RESIN MATERIALS: AN IN-VITRO STUDY

Sarita Singh*, Nitin Shah, Jyoti Mandlik, Manoj Nair, Shail Jaggi, Kalpana Kanyal

Dept. Of Conservative Dentistry and Endodontics, Bharati Vidyapeeth University, Dental College and Hospital, Pune, Maharashtra, INDIA

ABSTRACT

The present study was conducted to evaluate the effectiveness of various finishing and polishing procedures on the surface roughness of two different composite resin materials (nanofilled composite, microhybrid composite) and to evaluate the effect of the surface sealant application(prime and bond) on the surface roughness after finishing and polishing procedures of tested composites. A total of 60 composite discs of dimension 6 x 3 mm (6mm in diameter x 3mm in thickness) were made using a custom made stainless steel mould. Out of these sixty specimen, thirty were of nanofilled composite (Z-350 3M ESPE) and thirty were of microhybrid composite (Z-250 3M ESPE). These two groups were then again randomly divided into three subgroups for finishing and polishing by three different methods; Sof-Lex, Shofu and Mylar strip). The average surface roughness (Ra, µm) of all the specimen were measured with the profilometer. A surface sealant was then applied to all the treated specimens, according to manufacturer's instructions and the average roughness was measured again. Results were statistically analyzed using analysis of variance (ANOVA F) and the paired and unpaired't' tests. The results showed that irrespective of the finishing and polishing systems used nanofilled composite exhibited a smoother surface than microhybrid composite. As for the effectiveness of finishing and polishing systems on both the composites, the Mylar strips gave lowest Ra values followed by Sof-Lex followed by Shofu and the surface sealant improved the surface texture of tested specimens drastically.

Received on: 4th-Apr-2015
Revised on: 28th-June-2015
Accepted on: 20th-July-2015
Published on: 4th-Sept-2015

KEY WORDS

Microhybrid composite; Nanofilled composite; surface roughness; profilometer; surface sealant; finishing and polishing systems

***Corresponding author:** Email: drsaritavsingh@gmail.com **Tel:** +91-09765746178

INTRODUCTION

The esthetic quality of a restoration may be as important to the mental health of the patient as the biological and technical qualities of the restoration are to his physical and dental health. Use of composites in restorative dentistry has markedly increased in recent years due to increased demand of aesthetics [1].The surface quality is an important factor in determining the success of composite restorations[2]. Surface roughness is one reason for discoloration of restorations, and it is closely related to the type of composite material and the finishing and polishing systems used. Adequate finishing and polishing for composites is a prerequisite for high quality esthetics and enhanced longevity of restorations [3]. The composite restorations should be smooth so as to reduce plaque retention, surface staining, and recurrent decay.

The newer composites (for example microhybrid and nanofilled) combine the properties of hybrid composites and micro-filled composites. These systems have improved mechanical properties, better translucency and smoother surface finish. A variety of instruments are used for finishing and polishing composites. They remove the oxygen inhibited layer of resin but leave the surface rougher [4]. It is important to understand which type of surface-finishing treatments would be effective for different composite restorations. The present study evaluated the effectiveness of three different finishing and polishing systems in producing smoother surface finish of two different composite and the effectiveness of surface sealant application after finishing and polishing procedure of these composites.

THE IIOAB JOURNAL
ISSN: 0976-3104

MATERIALS AND METHODS

Specimen preparation

The resin composites used in this study were Z-350(nanofilled) and Z-250(microhybrid) of shade A3. The sealant used was "Prime and Bond" (Denstply). The three finishing and polishing system used in this study were "Shofu" finishing and polishing kit, "Sof-Lex "composite finishing and polishing kit (3M) and "Mylar Strips" (Unident). Sixty Cylindrical blocks of light-cured resin composite, 6mm in diameter and 3mm in depth, were prepared in a stainless steel mould. The stainless steel mould was placed on a glass slab and the composite to be tested was inserted in each cavity in a single increment using a resin packing plastic instrument. Excess flash of the material was removed. A Mylar Strip and glass slide was placed on the mould and the material was light cured from both the sides for 40 seconds using a Quartz-Tungsten-Halogen (QTH) light curing unit. The distance between the light source and the composite material in the mould was standardized. With this procedure, sixty composite discs (thirty of each composite; nanofilled and microhybrid) were obtained. All the specimens were then stored in distilled water at 37 ^{0}C for 24 hours in an incubator (Incubator (DBK BOD, Model - DTC 96, Innovative Bacteriological Incubator).

Finishing and polishing procedure, Sealant application and measurement of surface roughness

The thirty samples of each composite resin were then randomly subdivided into 3 subgroups (n= 10); to receive the finishing and polishing with Shofu, Sof-Lex and Mylar strip respectively. The specimens to be finished and polished with Shofu and Sof-Lex systems, for both the composites were surfaced with a Diamond finishing bur in a rotary motion, for 15 seconds with water coolant, to simulate initial finishing of the restorative material. The Mylar Strip groups of both the composite materials received no finishing and polishing treatment after being cured. The specimens of the two composite resins were finished and polished with the Sof-Lex system and Shofu system as specified by the manufacturer. After finishing and polishing, the surface roughness (Ra) of all the specimens was measured using a profilometer.

Further to evaluate the effect of surface sealant on the surface texture of all the finished and polished specimens, the Prime and Bond sealant was applied on all the specimens and again the surface roughness was measured using the profilometer. All the values of surface roughness obtained were subjected to statistical analysis. The data was analyzed with ANOVA F; paired and unpaired "t" test.

RESULTS

The results obtained from the statistical analysis indicate that the Mylar strip group showed smoothest surface texture for both the composites (nanofilled and microhybrid composite). Sof-Lex finishing and polishing system was better than the Shofu finishing and polishing system for both the composites. The surface texture for both the composites improved drastically after sealant application. Irrespective of the finishing and polishing system used, and whether or not the sealant was applied, the nanofilled composite showed lower surface values as compare to microhybrid composite (see **tables– 1, 2 and 3**).

Table– 1and 2 show the mean and standard deviation of surface roughness (Ra) values of both the composites. The values indicate that, for both the composites, the Mylar strip group shows lowest Ra values while Sof-Lex group shows lower Ra values than the Shofu group. For all the groups, in both the composites, the Ra values are less after sealant application indicating that the sealant application improved the surface texture

Table: 1. Comparison of surface roughness values for nanofilled composite treated with three systems before and after sealant application

	Z-350	N	Mean	SD	Paired t	P
Shofu	Before	10	0.8985	0.15621	2.619	.028 Sig
	After	10	0.8000	0.21546		
Sof-Lex	Before	10	0.7960	0.42589	1.355	0.208 NS
	After	10	0.6210	0.19564		
Mylar strip	Before	10	0.5510	0.23965	0.981	0.352 NS
	After	10	0.4890	0.17195		

Table: 2. Comparison of surface roughness values for microhybrid composite treated with three systems before and after sealant application

THE IIOAB JOURNAL
ISSN: 0976-3104

	Z-250	N	Mean	SD	Paired t	P
Shofu	Before	10	0.9320	0.17775	2.104	0.065 NS
	After	10	0.8610	0.12991		
Sof-Lex	Before	10	0.8570	0.42820	0.4	0.698 NS
	After	10	0.6210	0.19564		
Mylar strip	Before	10	0.4940	0.21910	2.235	0.052 NS
	After	10	0.4410	0.16763		

Table: 3. Comparison of Surface roughness between the materials

	Material	N	Mean	SD	Unpaired t	P
Before	Z-350	30	.7485	.32199	0.145	0.885 NS
	Z-250	30	.7610	.34562		
After	Z-350	30	.6367	.22861	1.113	0.270 NS
	Z-250	30	.7100	.27921		

Table– 3 compares the two resin materials, by the mean surface roughness values with their standard deviations, before and after sealant application. The values were analyzed by the unpaired 't' test. From this table it is observed that there is no statistically significant difference in the surface roughness values between the materials before and after sealant application. However, the mean Ra values for nanofilled composite (Z-350) are less than the microhybrid composite (Z-250) before and after sealant application.

DISCUSSION

Composite resins have been widely used since their introduction as they possess excellent aesthetic properties. Currently, composite resins are one of the most widely used materials in restorative dentistry having the widest range of indications. These resin materials have progressed from macrofills to microfills and from hybrid to microhybrids, and new materials such as packable and nanofilled composites have been introduced to the dental market. Each type of composite resin has certain advantages and limitations [5].

The universal hybrid composites provide the best general blend of good material properties and clinical performance for routine anterior and posterior restorations. Microhybrid and nanofilled composite resins exhibit low polymerization shrinkage, optimal handling properties and a durable polish. The average particle size of inorganic fillers in microhybrid dental composites has been reduced to around 1 µm or less so that the polished restoration can achieve adequate gloss and during long-term service, the wear of the restoration does not create a rough surface [5].

Nanofilled composite have been produced with nanofilled technology and formulated with nanomer and nanocluster filler particles. Nanomer are discrete nanoagglomerated particles of 20-75nm in size, and nanocluster are loosely bound agglomerates of nanosized particles. The combination of nanomer-sized particles and nanocluster formulations reduces the interstitial spacing of filler particles and, therefore, provides increased filler loading, better physical properties and superior polish and gloss retention [5].

Surface roughness is one reason for external discoloration, and it is closely related to the type of composite material and the finishing and polishing systems used. Hence adequate finishing and polishing for resin composite is a prerequisite for high quality esthetics and enhanced longevity of resin- based restorations [3]. The longevity and esthetics of a restoration greatly depends on the quality of finishing polishing techniques [6].

The finishing and polishing devices fall into one of three categories as coated abrasive, bonded abrasive or loose abrasives. Various motions may be critical to the development of optimal surface smoothness. A rotary motion, a planar motion and a reciprocating motion can be employed to polish the surface of resin based material. In rotary motion the axis of rotation is parallel to the surface being smoothened. The planar motion is a rotational movement with the axis of the rotation of the abrasive device perpendicular to the surface being smoothened. Reciprocating motion is employed when a finishing strip is pulled back and forth over a surface [6].

THE IIOAB JOURNAL
ISSN: 0976-3104

The present study compared the effectiveness of three finishing and polishing systems; Mylar strip, Shofu and Sof-Lex; on surface texture of two different composites, i.e., Microhybrid and Nanofilled composites. We also studied the influence of a sealant on the surface texture, applied after finishing and polishing procedure.

The results of this study show that the specimens polished with planar motion (Sof-Lex disks) gave lower surface roughness values than the specimens polished with rotary motion (Shofu) in both the composites. This is attributed to the Aluminium Oxide as an abrasive in Sof-Lex system. LS Turkun and M Turkun stated that the large particles embedded in Sof-Lex disks tend to rip through the surface of resin composite , when used with certain hybrid composites, tend to cut abrade filler particles resin matrix equally, resulting in a smooth surface [3]. For a composite finishing system to be effective the cutting particles (abrasive) must be relatively harder than the filler materials, otherwise the polishing agent will only remove a soft resin matrix and leave the filler particles protruding from the surface. The hardness of aluminium oxide is significantly higher than silicon dioxide, generally, higher than most filler materials used in composite formulations [7]. The trend of Sof-Lex discs is to provide a slightly smoother surface with the aluminium oxide abrasive on rigid matrix as this has the ability to flatten the filler particles and abrade the softer resin matrix at an equal rate.

In this study Mylar strips formed the smoothest surface in both the composite groups. The surface obtained with a Mylar strip is perfectly smooth and it is rich in resin organic binder. Therefore removal of outermost resin by finishing-polishing procedures would tend to produce a harder more wear resistant layer hence an esthetically stable surface [8]. Despite careful placement of matrices, removal of excess material and recontouring of restorations is often clinically necessary. This requires some degree of finishing and polishing that will violate the smoothness obtained with a matrix [4, 9].

The quantity and size of the fillers in composite resin greatly influences the surface characteristics of the final restoration. In composite resins in which fillers are markedly harder than the resin matrix the resin may suffer a preferential loss during finishing and polishing leaving the filler phase in positive relief. In several studies it was also reported that larger filler particle size resulted in greater roughness values. Use of composite resins with higher amount of small-sized filler particle content has increased in recent years due to difficulties in producing smooth surfaces such as enamel with composite resins which have larger particles. An increase in the amount of filler content results in smoother surface because of decreased particle size and better distribution within the resin matrix [10].

However even after accomplishing appropriate finishing and polishing technique, the surface of all resin composites exhibit micro- irregularities that inherently lead to material wear, deterioration and marginal infiltration resulting mainly from the abrasive processes to which the restoration is subjected in the oral environment. In an attempt to overcome this problem, using a thin layer of low viscosity resin over polymerized composite restoration has been investigated. This approach is assumed to provide a more uniform, regular surface, thereby, enhancing surface smoothness.

A sufficiently low-viscosity resin agent with proper characteristics and formulation, even though not specifically developed for such purpose, could be successfully used as a surface sealant .Various Studies have suggested coating polymerized resin composite with an adhesive agent or fissure sealant [11]. Rebonding of composite restoration with unfilled resin has been recommended for penetration of the sub-surface micro-cracks and interfacial gaps generated during finishing and polishing procedures [12]. In our study, surface sealing with Prime and Bond (Dentsply), had a positive effect on surface texture. The results of this study are in accordance with the results of studies by CYG Takuchi, EHG Lara, 2003 [11] and Nuray Attar 2007 [5].

CONCLUSIONS

Within the constraints of this in-vitro study, from the results obtained, we conclude that, though the surface roughness values of both the composite materials did not show statistically significant difference with all three finishing and polishing systems, the Mylar strips exhibited smoothest surface followed by Sof-Lex system. The Shofu system showed the highest surface roughness values for both the composite. As for the comparison between the Microhybrid and Nanofilled composites, the Nanofilled composite resin showed better surface texture with all the three finishing and polishing systems. Furthermore, the surface texture for both the composites improved drastically when sealant was applied after finishing and polishing procedures.

.

THE IIOAB JOURNAL
ISSN: 0976-3104

CONFLICT OF INTEREST

Authors declare no conflict of interest.

ACKNOWLEDGEMENT

I acknowledge the faculty of the department and laboratory persons involved in this study for their guidance and support.

FINANCIAL DISCLOSURE

The work was carried out without any financial support

REFERENCES

[1] Gupta R, Parkash H, Shah N, Jain V. [2005]A spectrophotometric evaluation of color changes of various tooth colored veneering materials after exposure to commonly consumed beverages. *JIPS* 5(2): 72−78.

[2] Uctasli MB, Arisu HD, Omurlu H, Eliguzeloglu E, Ozcan S, Ergun G. [2007]The effect of different finishing polishing systems on the surface roughness of different composite restorative materials. *J Contemp Dent Pract* 1;8 (2):89−96.

[3] LS Turkun, M Turkun. [2004] The effect of one-step polishing system on the surface roughness of three esthetic resin composite materials. *Operative Dentistry*, 29(2):203−211.

[4] E Ruyter. [1988]Composites - characterization of composite filling materials: reactor response. *Adv Dent Res* 2(1):122−129.

[5] Nuray Attar. [2007] The effect of finishing polishing procedures on the surface roughness of composite resin materials. *The Journal of Contemporary Practice* 8(1).

[6] Steven R Jefferies. [2007]Abrasive finishing polishing in restorative dentistry: a state-of-the-art review. *Dent Clin N Am* 51:379−397

[7] Reis AF, Giannini M, Lovadino JR, dos Santos Dias CT. [2002] The effect of six polishing systems on the surface roughness of two packable resin-based composites. *Am J Dent* 15: 193−197.

[8] Y Korkmaz, E Ozel, N Attar, G Aksoy. [2008]The influence of one-step polishing systems on the surface roughness microhardness of nanocomposites. *Operative Dentistry* 33(1): 44−50.

[9] AJ St- Georges, M Bolla, D Fortin. [2005]Surface finish produced on three resin composites by new polishing systems. *Operative Dentistry* 30(5): 593−597.

[10] AUJ Yap, JJ Ng, SH Yap, CK Teo. [2004]Surface finish of resin-modified highly viscous glass ionomer cements produced by new one-step systems. *Operative Dentistry* 29(1): 87−91.

[11] CYG Takeuchi, VH Orbegoso Flores, RG Palma Dibb, H Panzeri, EHG Lara, W Dinelli. [2003]Assessing the surface roughness of a posterior resin composite: Effect of surface sealing. *Operative Dentistry* 28(3): 283−288.

[12] M Jung, K Eichelberger J Klimek. [2007]Surface geometry of four nanofilled one composite after one-step multiple-step polishing. *Operative Dentistry* 32(4): 347−355.

ABOUT AUTHORS

***Sarita Singh**, MDS, Assistant Professor; Department of Conservative Dentistry and Endodontics at Bharati Vidyapeeth Deemed University Dental College and Hospital, Pune - 411 043, Maharashtra, INDIA*

***Dr. Nitin Shah** MDS, is the Head of Department of Conservative dentistry and Endodontics Bharati Vidyapeeth Deemed University Dental College and Hospital, Pune - 411 043, Maharashtra, INDIA*

***Dr. Jyoti Mandlik** MDS,, Associate Professor; Department of Conservative Dentistry and Endodontics at Bharati Vidyapeeth Deemed University Dental College and Hospital, Pune - 411 043, Maharashtra, INDIA*

***Dr. Manoj Nair ;MDS;** is post graduate teacher and guide; Department of Conservative Dentistry and Endodontics at Bharati Vidyapeeth Deemed University's Dental College and Hospital Pune, India*

***Dr. Shail Jaggi; MDS;** is post graduate teacher and guide; Department of Conservative Dentistry and Endodontics at Bharati Vidyapeeth Deemed University's Dental College and Hospital Pune, India*

***Kalpana Kanyal**, MDS, Assistant Professor; Department of Conservative Dentistry and Endodontics at Bharati Vidyapeeth Deemed University Dental College and Hospital, Pune - 411 043, Maharashtra, INDIA*